The Cryosphere

Discussions

Open Access

EGU

IcePAC – a Probabilistic Tool to Study Sea Ice Spatiotemporal Dynamic: Application to the Hudson Bay area, Northeastern Canada

Charles Gignac [1,2], Monique Bernier [1,2], Karem Chokmani [1,2]

5

[1] TENOR Laboratory, INRS – Eau Terre Environnement, Quebec City, G1K 9A9, Canada
[2] Centre for Northern Studies, Laval University, Quebec City, G1V 0A6, Canada

Correspondence to: Charles Gignac (Charles.Gignac@ete.inrs.ca)

Abstract. A reliable knowledge and assessment of the sea ice conditions and their evolution in time is a priority for

10   numerous decision makers in the domains of coastal and offshore management and engineering as well as in commercial navigation. As of today, countless research projects aimed at both modelling and mapping past, actual and future sea ice conditions were completed using sea ice numerical models, statistical models, educated guesses or remote sensing imagery. From these research, reliable information helping to understand sea ice evolution in space and in time are available to stakeholders. However, no research has, as of today, assessed the evolution of the sea ice cover with a frequency modelling

15   approach, by identifying the underlying theoretical distribution describing the sea ice behaviour at a given point in space and time. This project suggests the development of a probabilistic tool, named IcePAC, based on frequency modelling of historical 1978-2015 passive microwave sea ice concentrations maps from EUMETSAT OSI-409 product, to study the sea ice spatiotemporal behaviour in the waters of the Hudson Bay System in Northeastern Canada. Pixel scale models are based on the generalized Beta distribution and generated at a weekly temporal resolution. Results showed coherent with the

20   Canadian Ice Service 1980-2010 Sea Ice Climatic Atlas average freeze-up and meltdown dates for numerous coastal communities in the study area and showed that it is possible to evaluate a range of plausible events, such as the shortest and longest probable ice free season duration, for any given location on the simulation domain. Results obtained in this project open a path towards various analyses on sea ice dynamics that would gain in informative content and value by relying on the kind of probabilistic information and simulation data available from the IcePAC tool.

25   ## 1. Introduction

Numerous scientific projects recognized the link between climate change and changes in the spatiotemporal sea ice dynamics (Andrews et al., 2017; Cavalieri and Parkinson, 2012; Comiso, 2011, 2002; Comiso et al., 2008; Gloersen et al., 1998; Johannessen et al., 2004; Rothrock et al., 1999; Stocker, 2014; Stroeve et al., 2007; Stroeve et al., 2014; Stroeve et al., 2012; Wang and Overland, 2009). The average temperature raise in the Arctic region is said to reach 2.0°C according to

30   Serreze and Barry (2011), which makes it logical to apprehend that changes in the spatiotemporal dynamic of the sea ice cover will tend to amplify.

In this changing environment, an adequate and efficient monitoring of sea ice is of capital importance to better understand the climate and its impacts on marine and coastal areas (Allard and Champagne, 1980; Barnhart et al., 2014; Bernatchez and Dubois, 2004; Bernatchez and Dubois, 2008; Bintanja and Selten, 2014; Davies et al., 2014; Dionne, 1973;

35   Holland et al., 2006; Kowal et al., 2017; Manabe and Stouffer, 1995; Overeem et al., 2011; Peterson et al., 2002; Rahmstorf, 1995; Rahmstorf and Ganopolski, 1999; Vermaire et al., 2013), on the security of economical and logistical activities in northern communities (Aksenov et al., 2017; Andrews et al., 2017; Ho, 2010; Lasserre and Pelletier, 2011; Liu and Kronbak, 2010), on arctic marine fauna protection (Bhatt et al., 2010; Castro de la Guardia et al., 2013; Darnis et al., 2012; Laidre et al., 2015; Post et al., 2013; Wassmann et al., 2011) and on the traditional way of life of Inuit communities (Durkalec et al.,

40   2015; Laidler et al., 2010).

To understand and appreciate the role of the sea ice cover regarding climate, marine and coastal environment management, fauna protection and the cultural traditions of northern communities, access to informative and reliable sea ice dynamics information is fundamental. Engineers, stakeholders, Inuit and northern populations, navigators and scientists must be able to quantify hazards related to the sea ice cover in order to efficiently evaluate, anticipate and minimize the risks of

45   usage, building and exploitation in marine and coastal areas. Given the increase in activity noticed in the Arctic and the North, one can expect the demand in information to also increase.

Despite a large number of Earth observation datasets on the sea ice cover, only a few provide both high temporal and spatial resolutions. National ice services, such as the Canadian Ice Service (CIS), provide the users with sea ice conditions climatology that are a reliable source of descriptive statistics on the sea ice dynamics, such as the average freeze-up or

50   maximum extent date. Nevertheless, these datasets do not carry information on the nature of the underlying statistical distributions of sea ice parameters, such as sea ice concentration (SIC), at any given point and nor do they permit to analyse the probability of occurrence of a specific sea ice condition.

By exploring an innovative probabilistic sea ice concentrations modelling avenue, this study proposes a tool, named IcePAC, to characterize the underlying statistical distributions of the SIC at any point in the Hudson Bay System (Saucier et

55   al., 2004) based on historical passive microwave remote sensing data from 1978 to 2015. These data are than used to analyse the dynamic of SIC in the HBS with a probabilistic perspective and compared to the CIS climatology.
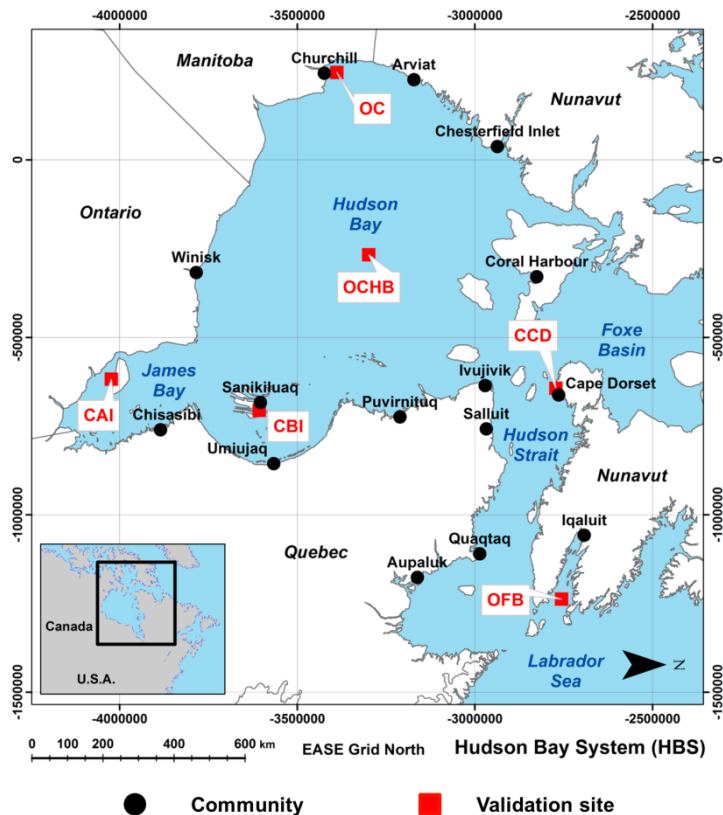
2. The Hudson Bay System

The study area is the Hudson Bay System, consisting of the Hudson Bay, the Hudson Strait, James Bay and Foxe Basin (Fig. 1). The HBS is surrounded by the three Canadian provinces of Quebec, Ontario, Manitoba and the territory of Nunavut.

60   It is the largest inland sea on Earth, with a total area of 1 300 000 km^2 (Etkin, 1991; Gagnon and Gough, 2005a; Martini, 1986) and is located in both subarctic and arctic regions. An estimated 20 % of the flux of freshwaters to the Arctic Ocean are thought to come from rivers flowing into the HBS, which represents 900 km^3/yr^{-1} (Déry and Wood, 2005; Déry and Wood, 2004). It is connected to the Labrador Sea by the Hudson Strait and to the Arctic Ocean by the Foxe Basin (Prinsenberg, 1986) and is characterized by shallow depths of less than 100 m in the Foxe Basin, of a maximum of 125 m in

65   the Hudson Bay and of more than 200 m in the Hudson Strait (Jones and Anderson, 1994). It has cyclonic currents generated mostly by winds, with a maximum intensity in November (Saucier et al., 2004).

A large number of researches have been done to document the average sea ice behavior in the HBS (CIS, 2013; Gagnon and Gough, 2005a, b; Hochheim and Barber, 2010; Hochheim and Barber, 2014; Kowal et al., 2017; Maxwell, 1986), which goes every year through a complete cryogenic cycle. The sea ice cover in the HBS is essentially constituted of first-year ice,

70   with the exception of possible multi-year ice drifting in the Foxe Basin (CIS, 2013; Etkin and Ramseier, 1993). The sea ice cover initially forms in the northwestern part of the HBS near Southampton Island in late November and progresses towards the southeastern part of the HBS (Hochheim and Barber, 2014; Maxwell, 1986) to finally achieve a complete freeze-up in late December. An annual maximum in extent is usually achieved in April (Gagnon and Gough, 2005b), after which the meltdown begins in May along the northwestern shoreline of the HBS. The meltdown is driven from the shores toward the

75   center of the Bay which usually results into an agglomerate of sea ice in the southern part of the Bay in late July (CIS, 2013). In summary, the HBS is on average entirely frozen in late December and entirely free of ice in mid-August (Mysak et al., 1996; Wang et al., 1994).

Figure 1: The Hudson Bay System with communities (black dots) and IcePAC validation sites (red squares)

3

3. Data and methods

Sea ice extent has displayed an important decline in the last decades (Cavalieri and Parkinson, 2012; Markus et al., 2009; Meier et al., 2007; Parkinson and Cavalieri, 2002, 2008; Parkinson et al., 1999), as it can be observed with remote sensing images acquired since 1978. Another important source of information on the sea ice cover are model predictions
85 which come from deterministic models (Hunke et al., 2017; Rousset et al., 2015; Weaver et al., 2001), based on dynamical and thermodynamic equations evolving in synergy inside a modelling framework, or from statistical models, based on statistical tools such as simple and multiple regression analysis (Ahn et al., 2014; Drobot, 2007; Pavlova et al., 2014) to explain an expected sea ice parameter value.

Another statistical approach, focusing on the estimation of the probabilities of occurrence of specific sea ice related
90 events, has been used in recent research. It is achieved either by using the simple count method (e.g. an event occurred four times int the last ten years, which corresponds to a 40 % probability of occurrence) or by using the frequency modelling method, which consist of adjusting a theoretical distribution to a series of observations, consequently defining the plausible sea ice events for the entire range of probabilities (i.e. p = 0 to 100 %). In this research, the frequency modelling method is used on series of passive microwave historical sea ice concentrations (SIC) remote sensing data to adjust distributions to a
95 total of 20 738 pixels or sites (i.e. the spatial dimension) for each of the 52 weeks of the year (i.e. the temporal dimension), resulting in a total of 1 078 376 distribution fits.

The datasets used and the protocols followed build the IcePAC tool and to model SIC distributions at every pixel in the HBS are described in the following section.

3.1 Sea ice concentration dataset

100 Sea ice concentration is defined as the proportion of sea ice covering a predefined area, expressed as a percentage (Shokr and Sinha, 2015). In remote sensing, this predefined area is represented by a pixel. The choice of an SIC dataset for frequency modelling in our study is highly influenced by the extent of the HBS (1 300 000 km^2) and has been made to ensure uniformity and continuity of the series used for analysis.

Multiple SIC datasets are generated using either visible/thermal, SAR or passive microwave remote sensing. As the
105 objective of the IcePAC tool is to provide the capacity to evaluate the spatiotemporal evolution of the SIC, the source of data needed to ensure a complete coverage of the HBS (i.e. the spatial dimension) and to ensure continuity in the series (i.e. the temporal dimension). A passive microwave dataset had been chosen as it answers these two needs.

The OSI-409 – Reprocessed Global Sea Ice Concentration dataset (Eastwood et al., 2015; Tonboe et al., 2016) was selected as it makes possible the reconstitution of SIC series on more than 30 years with a 12.5 km spatial resolution and is
110 processed with a unique hybrid SIC algorithm. The hybrid algorithm integrates the information taken from the Bootstrap algorithm (Comiso, 1995) when SIC < 70 %, linearly weights the SIC estimated by the Bootstrap and Bristol (Smith, 1996) algorithms when 70 % < SIC > 90 % and integrates the information from the Bristol algorithm when SIC > 90 %.

The data has been clipped to the HBS extent using Natural Earth (NaturalEarth, 2014) vector dataset with an estimated spatial resolution of 500 m (Wessel and Smith, 1996), well beyond the resolution of the OSI-409 data.

115   **3.2   Frequency modelling**

The core of the IcePAC tool relies on the use of frequency modelling which consist on describing the probable conditions at a given site with a simplified model fitted on historical SIC data, describing the underlying frequency distribution of the phenomenon. The first step in this approach is to build the time series of historical data, then to ensure their quality using preliminary tests and finally to identify and fit the model on the data (Fig. 2).
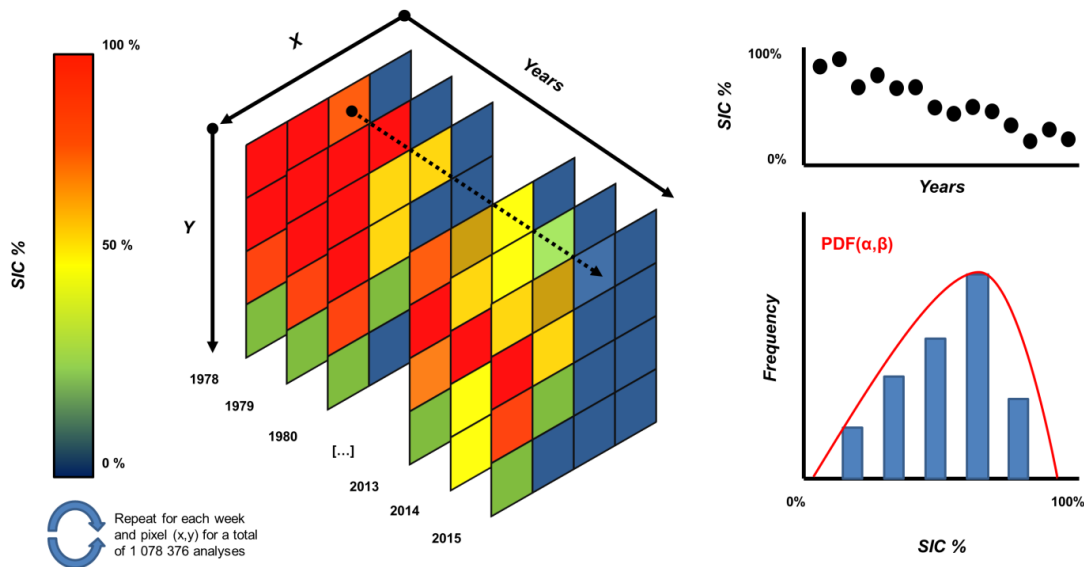
120

Figure 2: The process of frequency modelling from series building to model fit

3.2.1   Building the sea ice concentration (SIC) series

125   The SIC series are built to represent the SIC state for a specific week, for all years between 1978 and 2015. It is on these series that we adjust a theoretical distribution to estimate the probabilities of SIC related event. First, the daily OSI-409 data have to be averaged every 7 days to create weekly datasets. This operation is made following a 365-days "no-leap" calendar convention (i.e. every year has 365 days), separated in 52 weeks (December 31st is included in week 52). Second, the data for each week number are stacked in chronological order, from 1978 to 2015. Three types of series are observed in

130   the HBS (Fig. 3): the ICE series, where we observe constant high SIC, the MIZ (Marginal Ice Zone) series, where we observe a transition from sea ice to open water, and the OW (Open Water) series, where we observe constant low SIC.
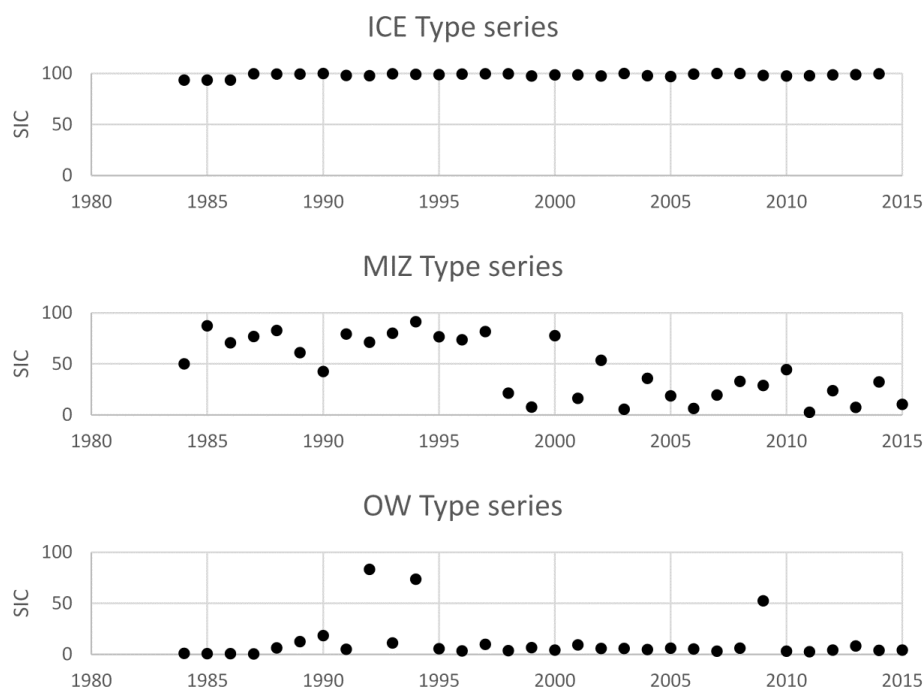
Figure 3: The three types of SIC series encountered in the HBS

135 **3.2.2   Preliminary tests**

Series have to go through a set of preliminary tests to assess their stationarity, homogeneity and independence, assuring they are suitable for frequency modelling. The tests used in IcePAC are the Mann-Kendall test for stationarity (Mann, 1945), the Wald-Wolfowitz test for independence (Wald and Wolfowitz, 1940) and the Wilcoxon test for homogeneity (Wilcoxon, 1945).

140   Series are considered independent if the subsequent unique SIC observations have no incidence on one another; they are considered homogeneous if they are reputed to be from the same distribution and; they are stationary if they are not affected by a trend. In the case of a detected non-stationarity, the trend must be modeled and subtracted from the series (Cave and Pearson, 1914).

All the time series, either original or detrended in regards to the Mann-Kendall test, satisfied the preliminary tests 145 for signification level of $\alpha = 0.05$.

3.2.3   Trend estimation and removal

The estimation of a trend on a percentage data series has the particularity that the trend must, in order to be coherent with the physics of the studied phenomenon, be bounded in a [0,1] domain (Baum, 2008). In other words, we must ensure we do not measure a trend that generates SIC values larger than 100 % or smaller than 0 %. To guarantee the respect of this 150 criterion, a generalized linear model with a logit link function has been used to estimate the trend. The logit link function

6

The Cryosphere

Discussions

Open Access

EGU

linearizes the SIC values using the logit transformation (Eq. 1) and it is on these transformed values that a linear regression of the form αx + β + ε is measured.

$$logit(SIC) = \ln(SIC/1 - SIC) \; where \; SIC \; is \; defined \; on \;]0,1[\tag{1}$$

155   For the trend to be removed from the series, an inverse transformation (Eq. 2) must be applied to the estimated trend to bring back its logit values into SIC values.

$$SIC = \exp\left(\frac{exp\big(logit(SIC)\big)}{\big(1 + exp\big(logit(SIC)\big)\big)}\right) \tag{2}$$

3.2.4   Distribution selection and fit

160   The selection of adequate candidate distributions to fit on the series is largely limited by the bounded nature of the data. The selected distribution has to be bounded to [0,1] and to be available in a generalized form in order to adapt to detrended series which are bounded to [-1,1]. Their generalized forms are to be used with the position parameter a fixed to -1 and the scale parameter b fixed at 2, in coherence with the phenomenon. It must also present enough flexibility in shape to adapt to the different type of SIC series in the HBS domain. Two different distributions, the generalized Beta distribution and Johnson's SB distribution (Johnson, 1949), both bounded and displaying flexibility in shape, have been fitted on the

165   series using the maximum likelihood estimator (MLE) (NIST, 2013) and compared by measuring the root mean square error between observations and adjusted curves as well as the Akaike Information Criterion (Akaike, 1998) and the Bayesian Information Criterion (Schwarz, 1978).

The generalized Beta distribution (Eq. 3) has four parameters which are the p (p > 0) and q (q > 0) shape

170   parameters, the position parameter a = -1 and the scale parameter b = 2. In Eq. 3, B is the Beta function. This distribution has been used before in climatology (Dirkson, 2017; Falls, 1974; Henderson-Sellers, 1978; Sulaiman et al., 1999), in seismology (Lallemant and Kiremidjian, 2015), to study air pollution (Nadarajah, 2008) and in hydrology (Chen and Singh, 2017; Yao, 1974).

$$f(x) = \frac{(x-a)^{p-1}(b-x)^{q-1}}{B(p,q)(b-a)^{p+q-1}}, where \; a \le x \le b; p, q > 0 \tag{3}$$

175

The Johnson's SB (Eq. 4) is, under its generalized form, a four parameters distribution, for which the γ and δ (δ > 0) are the shape parameters, the parameter a = -1 is position and the parameter b = 2 is the scale. This distribution has been used

before in meteorology (Cugerone and Michele, 2015; Wakazuki, 2013), in forestry (Rennolls and Wang, 2005) and in hydrology (D'Adderio et al., 2016).

180

$$f(x) = \frac{\delta}{\sqrt{2\pi}} \frac{(b-a)}{(x-a)(b-x)} \left[-\frac{1}{2}\left\{\gamma+\delta ln\left(\frac{x-a}{b-x}\right)\right\}^2\right], \text{where } b, \delta > 0 \tag{4}$$

Two approaches were tested for distribution selection. The first approach considered fitting the distributions to the series according to their Mann-Kendall test results. The second approach considered fitting the distributions to systematically detrended series in order to preserve spatial coherency in the IcePAC outputs.

185   The use of a systematic trend removal approach is justifiable by the fact that natural phenomena are considered by nature non stationary (Lins, 2012; Rao et al., 2012) and by the relative shortness of the series which can have an effect on the conclusions of the Mann-Kendall test (Hirsch et al., 1982).

The two approaches, tested on 958 randomly chosen series, brought similar conclusion, the Beta distribution outperforms the Johnson's SB distribution in 71.4 % of the time. For the remaining 28.6 % adjustments where the Johnson's

190   SB distribution did perform better, both the information criterion and the RMSE showed a non-significant difference with the Beta distribution. As expected, using an approach which systematically corrects for trends in series before distribution fit improved the spatial coherency of the resulting probability maps generated by IcePAC (Fig. 4). In scope of these results and to preserve parsimony in IcePAC, it was decided to use only the Beta distribution for all series, for which a systematic trend removal was applied.
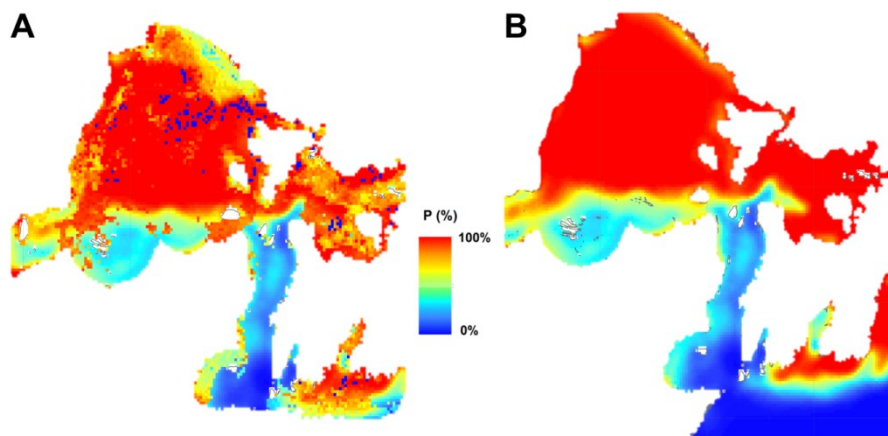
195

Figure 4: Comparison of IcePAC results for non-systematic (i.e. based on Mann-Kendall test result) trend removal (A) and systematic trend removal (B), on the resulting map for the probability of observing a SIC > 95% on week #1

3.2.5 Model queries

200   Queries with the IcePAC tool are possible via three important functions resulting from the distribution fit, the probability density function (PDF), the cumulative distribution function (CDF) and the percent point function (PPF). These functions are obtained using the fitted parameters from the Beta distribution independently for each of the 20 738 points.

The PDF is obtained by fitting a theoretical distribution on the frequency histogram of the SIC observations. The selected distribution in IcePAC is the Beta distribution for which the parameters of Eq. (3) were estimated using the

205   Maximum Likelihood Estimator (MLE). The PDF allows visualizing how the probability is distributed between values and how it evolves between different values.

Derived from the PDF, the CDF (Eq. 5) allows estimating the probability of a given range of SIC values. It corresponds to the area under the PDF curve for a specific range of SIC values, usually from 0 % to SIC_{MAX}. As a CDF example, one could query to know the probability of non-exceedance (p) for a sea ice concentration of 25 % (SIC_{MAX}) for

210   week #1 for the year to come.

$$F_x(SIC) = \int_0^{SIC_{MAX}} f_x(SIC)dt \qquad (5)$$

The inverse function of the CDF, the PPF (Eq. 6) allows to estimate the SIC value for a given probability of non-exceedance. As a PPF example, one could query to know the SIC_{MAX} for a probability of non-exceedance of 55 % for week

215   number 1 for the year to come.

$$Q = F^{-1}(p) \qquad (6)$$

Since the IcePAC fits are made on detrended series (e.g. residuals), the trend has to be taken into account when processing queries, meaning that it has to be either removed from the SIC_{MAX} value if the CDF is used or added to the result

220   of the PPF query in order to render a physically valid result. The query flowchart is presented in Fig. (5).
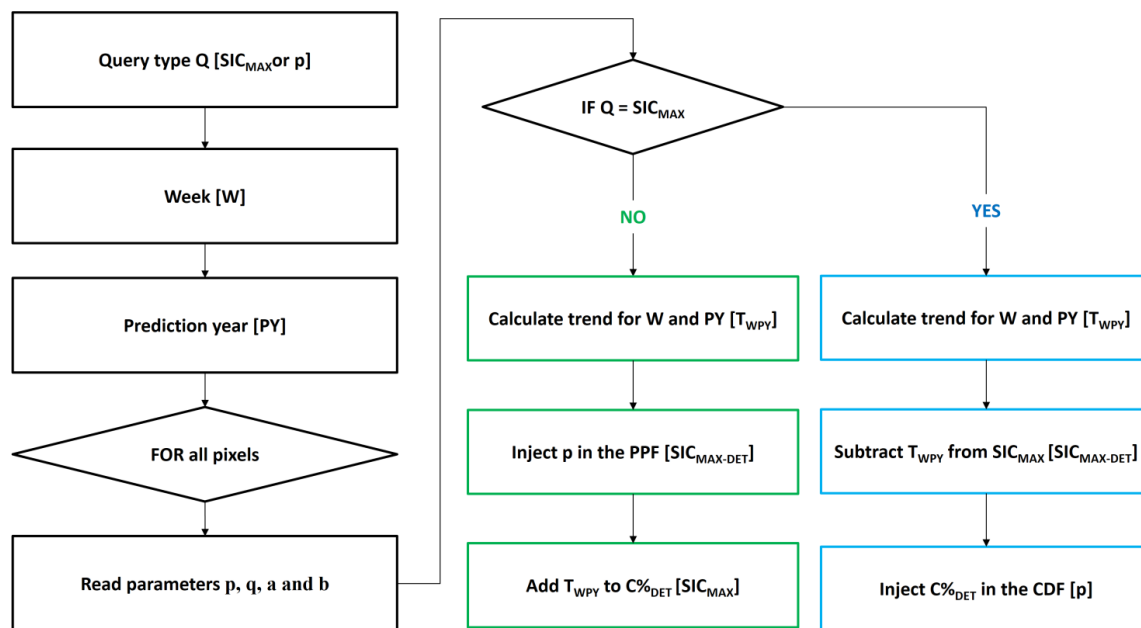
The Cryosphere
Discussions

Figure 5: IcePAC queries flowchart

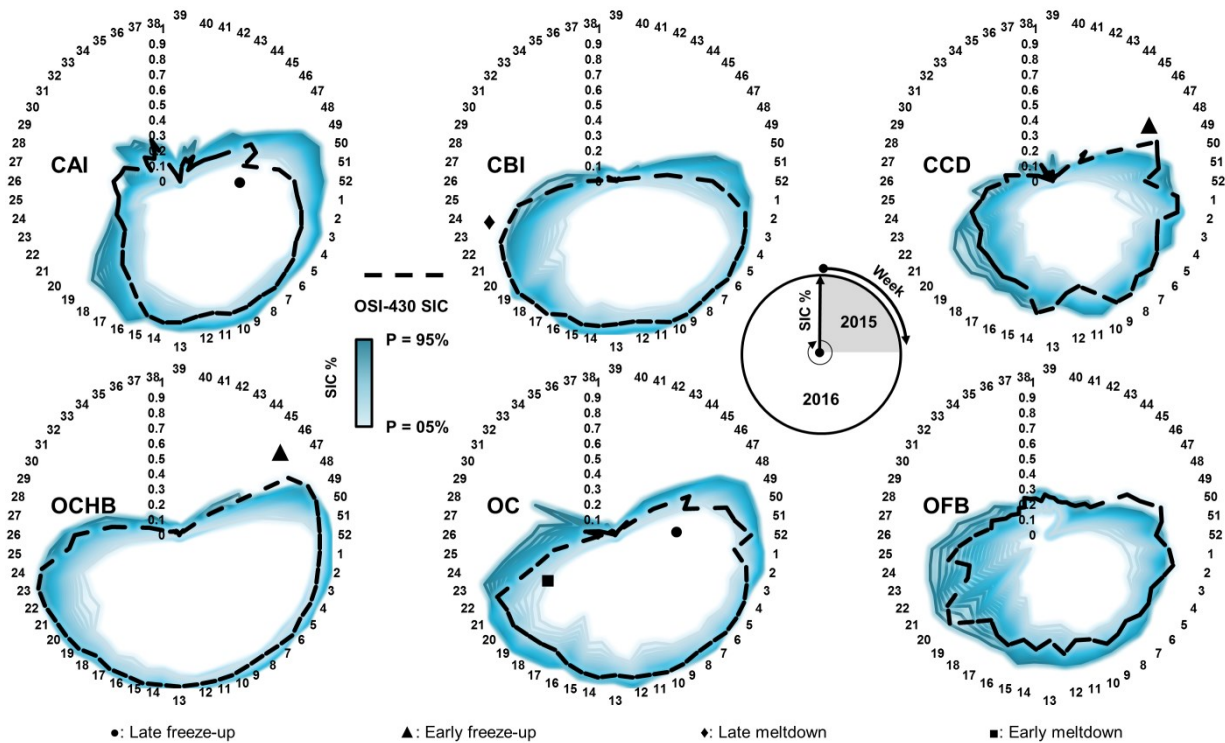### 3.2.6   IcePAC versus observations in 2016

225   The assessment of the validity of IcePAC predictions was done by comparing IcePAC weekly outputs time series
for the entire year with the OSI-430 product, an independent data source not used in IcePAC development but based on the
same SIC retrieval algorithm (Tonboe et al., 2016). The comparison was made on the 2015-2016 sea ice season, not included
in the input data used for fitting all underlying IcePAC Beta distributions.

     Six different comparison sites were selected to represent different sea ice dynamics (see Fig. 1). Three coastal sites,
230   the Akismi Island (CAI), Cape Dorset (CCD) and Belcher Islands (CBI), were sampled to assess the behavior of IcePAC
predictions along the coastline, at different latitudes. Also, three offshore sites, Frobisher Bay (OFB), Central Hudson Bay
(OCHB) and Churchill (OC) were sampled to assess the behavior of IcePAC predictions offshore, at different latitudes.

     Figure 6 displays weekly SIC predictions outputs from IcePAC, in the p = 5 to 95 % range with a 5 % pace. Each
comparison site shows a modeled dynamic which is coherent with reality and with the OSI-430 2015-2016 observation data.
235   As it could be expected, it is during the freeze-up and meltdown periods that the range of probable SIC values is the largest
(i.e. the spacing between light and dark blue lines in Fig. 6), compared to stable cover periods where the range of probable
SIC values narrows down. Variations in and out of the predicted range of SIC values can be attributed to the natural variation
of ice conditions, the occurrence of an highly improbable event, the OSI-409 algorithm bias or a combination of these
factors. Some anomalies of various intensities can be detected in the series such as: early 2015 freeze-up events at points

240   CCD and OCHB (▲ in Fig. 6); late 2015 freeze-up events at points CAI and OC (● in Fig. 6); late 2016 meltdown event at
point CBI (♦ in Fig. 6); and an early 2016 meltdown event at point OC (■ in Fig. 6), which all are in agreement with the
anomaly maps of the NSIDC's Arctic Sea Ice News and Analysis (https://nsidc.org/arcticseaicenews/) as well as anomaly
maps based on OSI-409.

Figure 6: IcePAC weekly outputs versus OSI-430 SIC observations for the 2015-2016 sea ice season

          The OFB point, near Iqaluit, has a behavior that indicates an underlying error. In fact, neither the predictions, nor
the observations reach a SIC value of 0 %, which is improbable in our study area. After an inquiry, the reason behind this
250   discrepancies with the validation data is that the OSI-409 product does not adequately estimate the SIC in this area, as it can
be seen in Fig. (7). The Frobisher Bay is usually ice free around mid-July, which is never the case in the OSI-409 dataset.
Possible sources of error include possible "land spill-over effect" (i.e. land contamination) on estimated SIC and the use of
the NSIDC sea ice monthly maximum extent climatology as a mask for restricting areas where sea ice is likely to occur.
Both of these bias sources are highly plausible explanations of the error detected in Frobisher Bay as the sensor resolution of
255   the passive microwave bands used in the OSI hybrid algorithm goes up to 56 km, which is larger than some parts of
Frobisher Bay and as the NSIDC climatology maps indicate Frobisher Bay as potentially frozen during the summer month,
which is erroneous as a comparison with MODIS data confirms.
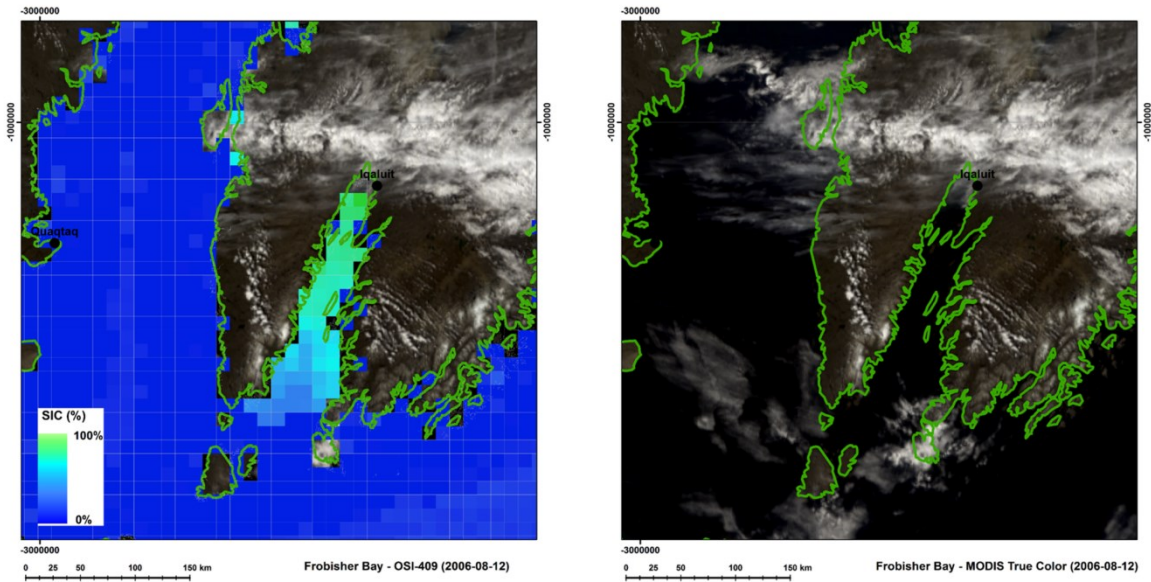
Figure 7: Frobisher Bay OSI-409 error and time concordant MODIS True Color composite

Such errors make it important to emphasize that the results obtained from the model are to be used with care and ideally in combination with other sources of information such as local knowledge, other remote sensing imagery and historical sea ice maps from national sea ice services.

4. Analysis of Hudson Bay sea ice spatiotemporal dynamic

The major asset of the IcePAC tool is that its output data gives a probabilistic perspective on relevant sea ice event, comparatively to the usual static descriptive statistics. Therefore, IcePAC gives not only the capacity to determine the mean event, but also to estimate the range of plausible events for a given site and date.

Here, the IcePAC outputs are used to assess the sea ice spatiotemporal dynamic given different probability scenarios and in terms of three cover indicators which are the length of the ice free season (or its corollary the ice covered season), the probable complete melt week and the probable complete freeze-up week.

4.1 Analysis with the IcePAC tool

Before presenting any results, the ice indicators analyzed in the next paragraphs must be clearly defined. First, the probable complete melt week corresponds to, for varying probability scenarios, to the first week for which the SIC is below 15 % at a given pixel. Second, the probable complete freeze-up week corresponds to, for varying probability scenarios, to the

The Cryosphere
Discussions

first week for which the SIC is above 15 % at a given pixel. Finally, the probable duration of the ice free season corresponds to the gap, in weeks, between the different probable meltdown and freeze-up weeks.

The use of the 15 % limit to define presence or absence of sea ice is a convention used by many authors (Andersen et al., 2006; Cavalieri et al., 1997; Cavalieri et al., 1999; Divine and Dick, 2006; Gloersen et al., 1993; Pang et al., 2018) for 280 SIC derived with passive microwave data and was therefore used in this analysis.

To estimate the aforementioned ice indicators, the probable SIC value for a given non-exceedance probability (p) was extracted from IcePAC for every location and week. For this analysis, a range of non-exceedance probabilities going from 5 % to 95 % were evaluated, with a step of 5 % between each analysis. Time series of the results were compiled and it is on these series that the complete freeze-up and meltdown events were identified. Figure 8 shows the estimated freeze-up and 285 meltdown events weeks for p = 50 %.

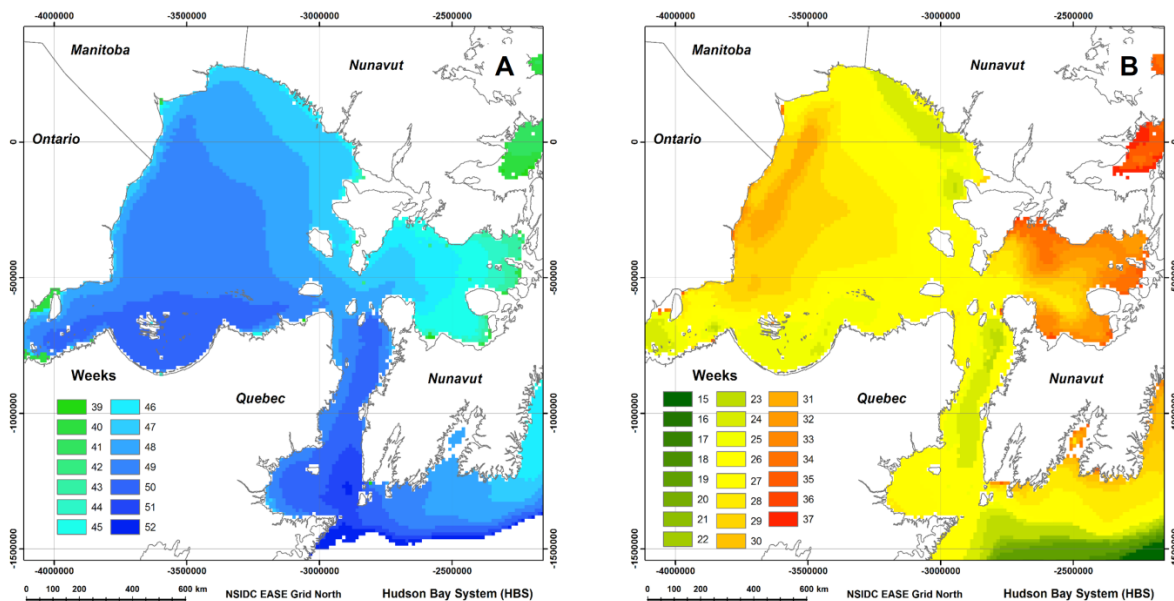**Figure 8:** Estimated freeze-up (A) and meltdown (B) weeks for p=50 % in the HBS

290 This detection process was repeated for every of the 20 738 pixels of the domain and for each probability step. It is worth to note that while the meltdown is described as a non-exceedance event (SIC < 15 %), directly deducted from p, the freeze-up is actually defined as an exceedance event (SIC > 15 %), deducted from 1-p.

Figure 9A presents the probable freeze-up and meltdown events for the coastal community of Puvirnituq, located in the northeastern part of the Hudson Bay. In this figure we notice that meltdown has a 25% probability to be completed by 295 week 25 (Jun. 18th to Jun. 24th), only a 10% probability of being completed for week 24 (Jun. 11th to Jun. 17th) and is certain to be completed by week 31 (Jul. 30th to Aug. 05th). According to the two curves plotted in Fig. (9A), we can state that a

13

complete freeze-up and complete meltdown at Puvirnituq can be respectively expected, with a very high probability of occurrence (p > 95 %) on weeks 50 (Dec. 10th to Dec. 16th) and 31 (Jul. 30th to Aug. 05th). Figure 9B shows an assessment of the range of probable ice free season duration made for the same coastal community. Here, the freeze-up curve is inversed

300   (1-P) as the shortest possible ice free season duration is a combination of the latest possible meltdown (high exceedance probability) and the earliest possible freeze-up (high non-exceedance probability). By comparing the space between the two curves for the 5 % to 95 % probability range, we observe that the shortest possible ice free season at Puvirnituq is of 14 weeks and that the longest is of 26 weeks. Figure 9C shows the ice free season duration estimated for numerous coastal communities located in the study area using the method described for Fig. (9B). Particularly remarkable cases can be noticed

305   such as Cape Dorset, which displays a large variability in possible ice free season duration given the polynya located along the coast in front of the community and Winisk, located in the southcentral part of the Hudson Bay, where ice tends to form early and melt late, which explains the shorter ice free seasons when compared to other communities.
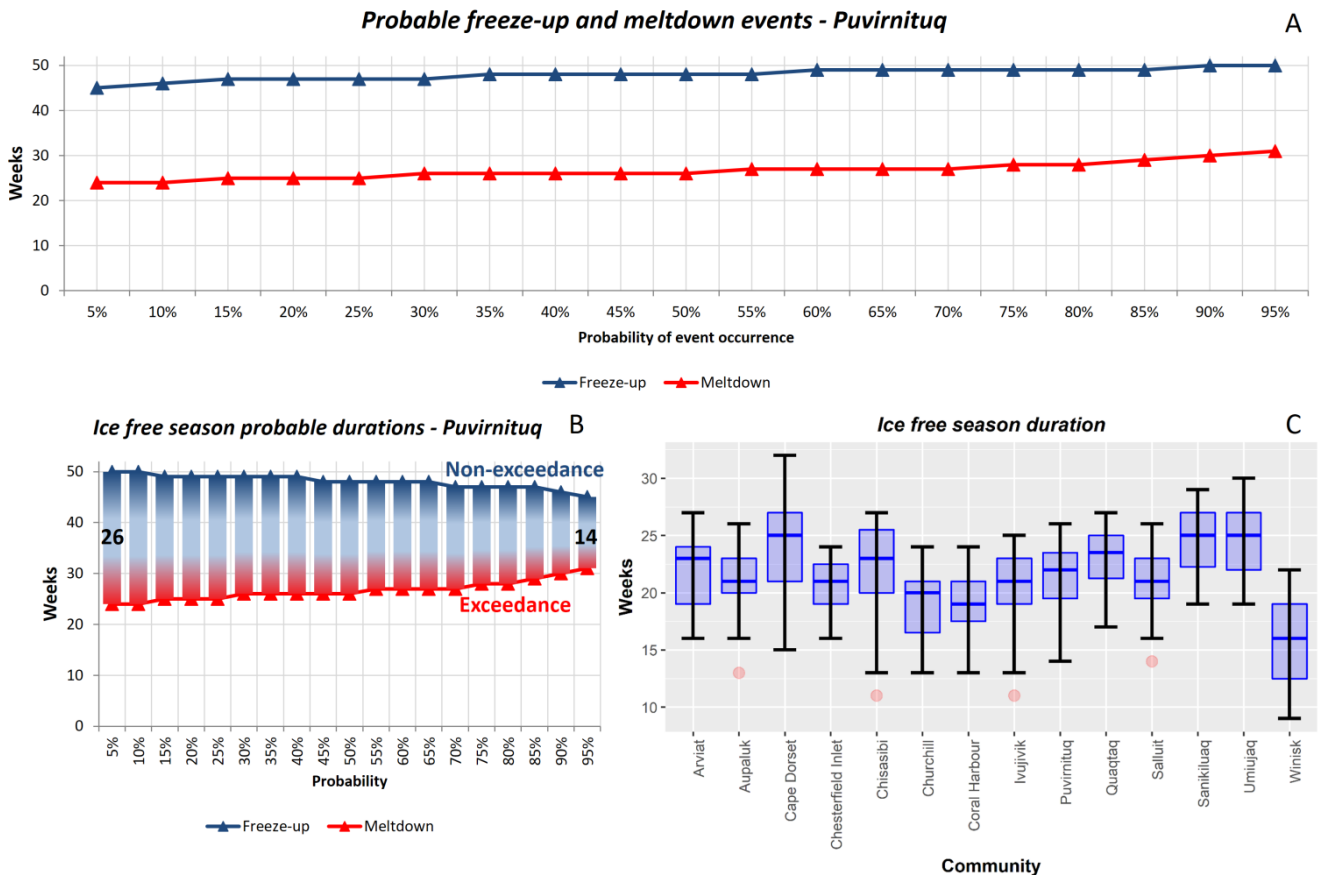
310   **Figure 9:** Probable freeze-up and meltdown events for the coastal community of Puvirnituq (A), range of probable ice free season duration for the same community (B) and probable ice free season lengths for all coastal communities of the HBS (C)

The Cryosphere
Discussions

4.2 Comparison with the Canadian Ice Service Atlas

The HBS has been under scrutiny for many decades by the Canadian Ice Service (CIS) and they have gathered numerous sea ice conditions maps in the area from which they built a 30 years sea ice climatological atlas (CIS, 2013),
315 portraying the average sea ice conditions, freeze-up and melting dates. As the information provided by the CIS atlas is given based on average values, a comparison with the p = 50 % IcePAC output gives an outlook on the coherency of the model when compared with another source of data, built around a different methodology. The comparison, as displayed in Table 1, confirms that the freeze-up and melting dates identified by IcePAC are realistic when compared to the CIS historical data. Small differences in weeks are present and may be linked to a multitude of factors, the most important being the different
320 methodologies used to generate the data. The CIS atlas is based on ice maps made by trained sea ice analysts and calculated with descriptive statistics while IcePAC is based on algorithmically generated ice maps and calculated from adjusted frequency models. Also, there is a difference in spatial resolution between the two products; CIS uses mostly Synthetic Aperture Radar (SAR) images at 50 m resolution while IcePAC uses passive microwave images resampled at 12.5 km resolution. Finally, there is a timeframe difference as the CIS atlas is built with data from 1980-2010 (30 years) while
325 IcePAC is built with data from 1978-2015 (37 years).

Table 1: Comparison between the CIS atlas and IcePAC p = 50 % modeled occurrence weeks for the freeze-up and meltdown events at selected sites in the HBS. (F = Freeze-up, M = Melting)

COMMUNITY	CIS (F)	CIS (M)	P=50% (F)	P=50 % (M)	DIFF. (F)	DIFF. (M)
Arviat	47	25	47	24	0	1
Aupaluk	48	28	48	27	0	1
Cape Dorset	49	24	49	24	0	0
Chesterfield Inlet	47	25	46	25	1	0
Chisasibi	NA*	27	49	26	NA*	1
Churchill	47	27	47	27	0	0
Coral Harbour	45	26	46	27	-1	-1
Ivujivik	48	25	48	27	0	2
Puvirnituq	48	25	48	26	0	-1
Quaqtaq	48	25	49	25	-1	0
Salluit	49	24	48	26	-1	-2
Sanikiluaq	48	25	50	25	-2	0
Umiujaq	49	25	50	25	-1	0
Winisk	46	30	47	31	-1	-1

* NA = Not covered by Canadian Ice Service 30 years sea ice atlas

15

The Cryosphere
Discussions
Open Access
EGU

5. Conclusion

330

The IcePAC tool permits an assessment of plausible sea ice related events for the entire range of probabilities for 20 738 sites (pixels) in the Hudson Bay System, for all 52 weeks of the year. It is based on local (pixel) models that use the generalized Beta distribution to describe the sea ice behaviour with four parameters at each site (with position and scale being fixed), based on historical 1978-2015 information from passive microwave imagery (OSI-409). From these

335 parameters, IcePAC generates spatialized sea ice probabilistic information that can be used in any geographic information system or a web based map interface for further analyses.

An analysis has been made to define, for each pixel in the simulation domain, the plausible scenarios for each probability. A subsequent comparison with 1980-2010 Canadian Ice Service sea ice climatology atlas (CIS, 2013) showed that the information generated with the IcePAC tool, for the p = 50 % case, renders coherent probabilities for freeze-up and

340 meltdown events all over the HBS. Another analysis, focused the community of Puvirnituq, showed that it is possible to evaluate locally the "worst" and "best" case scenarios in term of ice free season length.

The model outputs generated with the IcePAC tool are bringing a novel probabilistic perspective regarding important events related to sea ice dynamics that was not available before. With its capacity to be transposed to other areas and to be easily updated, the IcePAC tool brings information on probable freeze-up and meltdown weeks as well as on ice presence

345 and ice free season lengths. This relevant information will help decision makers apprehend the possible scenarios of sea ice dynamics and to prepare for an effective mitigation of climate change impacts on the coastal and offshore environments.

Author Contribution

CG defined the objectives of this research project, processed the data, coded the IcePAC tool, analysed the results and wrote this research paper. MB and KC participated in defining the objectives, guiding the development of the tool, analysing the

350 results and writing this paper.

Competing Interests

The authors declare no conflicts of interest.

References

Ahn, J., Hong, S., Cho, J., Lee, Y.-W., and Lee, H.: Statistical Modeling of Sea Ice Concentration Using Satellite Imagery and Climate Reanalysis Data in the Barents and Kara Seas, 1979–2012, Remote Sensing, 6, 5520, 2014.

360 Akaike, H.: Information theory and an extension of the maximum likelihood principle. In: Selected Papers of Hirotugu Akaike, Springer, 1998.

Aksenov, Y., Popova, E. E., Yool, A., Nurser, A. J. G., Williams, T. D., Bertino, L., and Bergh, J.: On the future navigability of Arctic sea routes: High-resolution projections of the Arctic Ocean and sea ice, Marine Policy, 75, 300-317, 2017.

Allard, M. and Champagne, P.: Dynamique glacielle à la pointe d'Argentenay, île d'Orléans, Québec, Géographie physique et Quaternaire, 34, 159-174, 1980.
365

Andersen, S., Tonboe, R., Kern, S., and Schyberg, H.: Improved retrieval of sea ice total concentration from spaceborne passive microwave observations using numerical weather prediction model fields: An intercomparison of nine algorithms, Remote Sensing of Environment, 104, 374-392, 2006.

Andrews, J., Babb, D., and Barber, D. G.: Climate change and sea ice: Shipping accessibility on the marine transportation corridor through Hudson Bay and Hudson Strait (1980–2014), Elem Sci Anth, 5, 2017.
370

Barnhart, K. R., Overeem, I., and Anderson, R. S.: The effect of changing sea ice on the physical vulnerability of Arctic coasts, The Cryosphere, 8, 1777-1799, 2014.

Baum, C. F.: Stata tip 63: Modeling proportions, Stata Journal, 8, 299, 2008.

Bernatchez, P. and Dubois, J.-M.: Bilan des connaissances de la dynamique de l'érosion des côtes du Québec maritime laurentien, Géographie physique et Quaternaire, 58, 45-71, 2004.
375

Bernatchez, P. and Dubois, J.-M. M.: Seasonal Quantification of Coastal Processes and Cliff Erosion on Fine Sediment Shorelines in a Cold Temperate Climate, North Shore of the St. Lawrence Maritime Estuary, Québec, Journal of Coastal Research, 24, 169-180, 2008.

Bhatt, U. S., Walker, D. A., Raynolds, M. K., Comiso, J. C., Epstein, H. E., Jia, G., Gens, R., Pinzon, J. E., Tucker, C. J., Tweedie, C. E., and Webber, P. J.: Circumpolar Arctic Tundra Vegetation Change Is Linked to Sea Ice Decline, Earth Interactions, 14, 1-20, 2010.
380

Bintanja, R. and Selten, F. M.: Future increases in Arctic precipitation linked to local evaporation and sea-ice retreat, Nature, 509, 479, 2014.

Castro de la Guardia, L., Derocher, A. E., Myers, P. G., Terwisscha van Scheltinga, A. D., and Lunn, N. J.: Future sea ice conditions in Western Hudson Bay and consequences for polar bears in the 21st century, Global Change Biology, 19, 2675-2687, 2013.
385

Cavalieri, D. J., Gloersen, P., Parkinson, C. L., Comiso, J. C., and Zwally, H. J.: Observed Hemispheric Asymmetry in Global Sea Ice Changes, Science, 278, 1104-1106, 1997.

Cavalieri, D. J. and Parkinson, C. L.: Arctic sea ice variability and trends, 1979–2010, The Cryosphere, 6, 881-889, 2012.

390 Cavalieri, D. J., Parkinson, C. L., Gloersen, P., Comiso, J. C., and Zwally, H. J.: Deriving long-term time series of sea ice cover from satellite passive-microwave multisensor data sets, Journal of Geophysical Research: Oceans, 104, 15803-15814, 1999.

Cave, B. M. and Pearson, K.: Numerical illustrations of the variate difference correlation method, Biometrika, 10, 340-355, 1914.

395 Chen, L. and Singh, V. P.: Generalized beta distribution of the second kind for flood frequency analysis, Entropy, 19, 254, 2017.

CIS: https://ec.gc.ca/glaces-ice/default.asp?lang=En&n=4B35305B-1, 2013.

Comiso, J. C.: Large Decadal Decline of the Arctic Multiyear Ice Cover, Journal of Climate, 25, 1176-1193, 2011.

Comiso, J. C.: A rapidly declining perennial sea ice cover in the Arctic, Geophysical Research Letters, 29, 2002.

400 Comiso, J. C.: SSM/I sea ice concentrations using the bootstrap algorithm, National Aeronautics and Space Administration, Goddard Space Flight Center, 1995.

Comiso, J. C., Parkinson, C. L., Gersten, R., and Stock, L.: Accelerated decline in the Arctic sea ice cover, Geophysical research letters, 35, 2008.

Cugerone, K. and Michele, C. D.: Johnson SB as general functional form for raindrop size distribution, Water Resources
405 Research, 51, 6276-6289, 2015.

D'Adderio, L. P., Cugerone, K., Porcù, F., De Michele, C., and Tokay, A.: Capabilities of the Johnson SB distribution in estimating rain variables, Advances in Water Resources, 97, 241-250, 2016.

Darnis, G., Robert, D., Pomerleau, C., Link, H., Archambault, P., Nelson, R. J., Geoffroy, M., Tremblay, J.-É., Lovejoy, C., Ferguson, S. H., Hunt, B. P. V., and Fortier, L.: Current state and trends in Canadian Arctic marine ecosystems: II.
410 Heterotrophic food web, pelagic-benthic coupling, and biodiversity, Climatic Change, 115, 179-205, 2012.

Davies, F. J., Renssen, H., and Goosse, H.: The Arctic freshwater cycle during a naturally and an anthropogenically induced warm climate, Climate Dynamics, 42, 2099-2112, 2014.

Déry, S. J. and Wood, E. F.: Decreasing river discharge in northern Canada, Geophysical Research Letters, 32, 2005.

Déry, S. J. and Wood, E. F.: Teleconnection between the Arctic Oscillation and Hudson Bay river discharge, Geophysical
415 Research Letters, 31, 2004.

Dionne, J.-C.: La notion de pied de glace (Icefoot), en particulier dans l'estuaire du Saint-Laurent, Cahiers de géographie du Québec, 17, 221-250, 1973.

Dirkson, A.: Initializing sea ice thickness and quantifying uncertainty in seasonal forecasts of Arctic sea ice, 2017. 2017.

Divine, D. V. and Dick, C.: Historical variability of sea ice edge position in the Nordic Seas, Journal of Geophysical
420 Research: Oceans, 111, 2006.

Drobot, S. D.: Using remote sensing data to develop seasonal outlooks for Arctic regional sea-ice minimum extent, Remote Sensing of Environment, 111, 136-147, 2007.

Durkalec, A., Furgal, C., Skinner, M. W., and Sheldon, T.: Climate change influences on environment as a determinant of Indigenous health: Relationships to place, sea ice, and health in an Inuit community, Social Science & Medicine, 136-137, 425   17-26, 2015.

Eastwood, S., Jenssen, M., Lavergne, T., Sorensen, A., and Tonboe, R.: Global Sea Ice Concentration Reprocessing - Product User Manual, EUMETSAT - OSISAF, User guide, 29 pp., 2015.

Etkin, D. A.: Break-up in Hudson Bay: its sensitivity to air temperatures and implications for climate warming, Climatological Bulletin, 25, 21-34, 1991.

430   Etkin, D. A. and Ramseier, R. O.: A comparison of conventional and passive microwave sea-ice datasets for Hudson Bay, Atmosphere-Ocean, 31, 359-378, 1993.

Falls, L. W.: The beta distribution: a statistical model for world cloud cover, Journal of Geophysical Research, 79, 1261-1264, 1974.

Gagnon, A. S. and Gough, W. A.: Climate Change Scenarios for the Hudson Bay Region: An Intermodel Comparison, 435   Climatic Change, 69, 269-297, 2005a.

Gagnon, A. S. and Gough, W. A.: Trends in the dates of ice freeze-up and breakup over Hudson Bay, Canada, Arctic, 2005b. 370-382, 2005b.

Gloersen, P., Campbell, W. J., Cavalieri, D. J., Comiso, J. C., Parkinson, C. L., and Zwally, H. J.: Satellite passive microwave observations and analysis of Arctic and Antarctic sea ice, 1978–1987, Annals of Glaciology, 17, 149-154, 1993.

440   Gloersen, P., Parkinson, C. L., Cavalieri, D. J., Cosmiso, J. C., and Zwally, H. J.: Spatial Distribution of Trends and Seasonality in the Hemispheric Sea Ice Covers, 1998. 1998.

Henderson-Sellers, A.: Surface type and its effect upon cloud cover: A climatological investigation, Journal of Geophysical Research: Oceans, 83, 5057-5062, 1978.

Hirsch, R. M., Slack, J. R., and Smith, R. A.: Techniques of trend analysis for monthly water quality data, Water resources 445   research, 18, 107-121, 1982.

Ho, J.: The implications of Arctic sea ice decline on shipping, Marine Policy, 34, 713-715, 2010.

Hochheim, K. and Barber, D.: Atmospheric forcing of sea ice in Hudson Bay during the fall period, 1980–2005, Journal of Geophysical Research: Oceans, 115, 2010.

Hochheim, K. P. and Barber, D. G.: An update on the ice climatology of the Hudson Bay system, Arctic, antarctic, and 450   alpine research, 46, 66-83, 2014.

Holland, M. M., Finnis, J., and Serreze, M. C.: Simulated Arctic Ocean Freshwater Budgets in the Twentieth and Twenty-First Centuries, Journal of Climate, 19, 6221-6242, 2006.

Hunke, E., Lipscomb, W., Jones, P., Turner, A., Jeffery, N., and Elliott, S.: CICE, The Los Alamos Sea Ice Model, Los Alamos National Laboratory (LANL), Los Alamos, NM (United States), 2017.

455 Johannessen, O. M., Bengtsson, L., Miles, M. W., Kuzmina, S. I., Semenov, V. A., Alekseev, G. V., Nagurnyi, A. P., Zakharov, V. F., Bobylev, L. P., and Pettersson, L. H.: Arctic climate change: Observed and modelled temperature and sea-ice variability, Tellus A, 56, 328-341, 2004.

Johnson, N. L.: Systems of frequency curves generated by methods of translation, Biometrika, 36, 149-176, 1949.

Jones, E. P. and Anderson, L. G.: Northern Hudson Bay and Foxe Basin: water masses, circulation and productivity,
460 Atmosphere-Ocean, 32, 361-374, 1994.

Kowal, S., Gough, W. A., and Butler, K.: Temporal evolution of Hudson Bay Sea Ice (1971–2011), Theoretical and Applied Climatology, 127, 753-760, 2017.

Laidler, G. J., Elee, P., Ikummaq, T., Joamie, E., and Aporta, C.: Mapping Inuit Sea Ice Knowledge, Use, and Change in Nunavut, Canada (Cape Dorset, Igloolik, Pangnirtung). In: SIKU: Knowing Our Ice: Documenting Inuit Sea Ice Knowledge
465 and Use, Krupnik, I., Aporta, C., Gearheard, S., Laidler, G. J., and Kielsen Holm, L. (Eds.), Springer Netherlands, Dordrecht, 2010.

Laidre, K. L., Stern, H., Kovacs, K. M., Lowry, L., Moore, S. E., Regehr, E. V., Ferguson, S. H., Wiig, Ø., Boveng, P., and Angliss, R. P.: Arctic marine mammal population status, sea ice habitat loss, and conservation recommendations for the 21st century, Conservation Biology, 29, 724-737, 2015.

470 Lallemant, D. and Kiremidjian, A.: A Beta Distribution Model for Characterizing Earthquake Damage State Distribution, Earthquake Spectra, 31, 1337-1352, 2015.

Lasserre, F. and Pelletier, S.: Polar super seaways? Maritime transport in the Arctic: an analysis of shipowners' intentions, Special section on Alternative Travel futures, 19, 1465-1473, 2011.

Lins, H. F.: A note on stationarity and nonstationarity. Hydrology, W. C. f. (Ed.), 2012.

475 Liu, M. and Kronbak, J.: The potential economic viability of using the Northern Sea Route (NSR) as an alternative route between Asia and Europe, Tourism and climate change, 18, 434-444, 2010.

Manabe, S. and Stouffer, R. J.: Simulation of abrupt climate change induced by freshwater input to the North Atlantic Ocean, Nature, 378, 165, 1995.

Mann, H. B.: Nonparametric Tests Against Trend, Econometrica, 13, 245-259, 1945.

480 Markus, T., Stroeve, J. C., and Miller, J.: Recent changes in Arctic sea ice melt onset, freezeup, and melt season length, Journal of Geophysical Research: Oceans (1978–2012), 114, 2009.

Martini, I. P.: Coastal features of Canadian inland seas. In: Elsevier oceanography series, Elsevier, 1986.

Maxwell, J. B.: A climate overview of the Canadian inland seas. In: Elsevier oceanography series, Elsevier, 1986.

Meier, W. N., Stroeve, J., and Fetterer, F.: Whither Arctic sea ice? A clear signal of decline regionally, seasonally and
485 extending beyond the satellite record, Annals of Glaciology, 46, 428-434, 2007.

Mysak, L. A., Ingram, R. G., Wang, J., and Van Der Baaren, A.: The anomalous sea-ice extent in Hudson Bay, Baffin Bay and the Labrador Sea during three simultaneous NAO and ENSO episodes, Atmosphere-Ocean, 34, 313-343, 1996.

Nadarajah, S.: A truncated inverted beta distribution with application to air pollution data, Stochastic Environmental Research and Risk Assessment, 22, 285-289, 2008.

490   NaturalEarth: Coastline. NaturalEarth (Ed.), 2014.

NIST: https://www.itl.nist.gov/div898/handbook/index.htm, 2013.

Overeem, I., Anderson, R. S., Wobus, C. W., Clow, G. D., Urban, F. E., and Matell, N.: Sea ice loss enhances wave action at the Arctic coast, Geophysical Research Letters, 38, 2011.

Pang, X., Pu, J., Zhao, X., Ji, Q., Qu, M., and Cheng, Z.: Comparison between AMSR2 Sea Ice Concentration Products and
495   Pseudo-Ship Observations of the Arctic and Antarctic Sea Ice Edge on Cloud-Free Days, Remote Sensing, 10, 317, 2018.

Parkinson, C. L. and Cavalieri, D. J.: A 21 year record of Arctic sea-ice extents and their regional, seasonal and monthly variability and trends, Annals of Glaciology, 34, 441-446, 2002.

Parkinson, C. L. and Cavalieri, D. J.: Arctic sea ice variability and trends, 1979–2006, Journal of Geophysical Research: Oceans, 113, n/a-n/a, 2008.

500   Parkinson, C. L., Cavalieri, D. J., Gloersen, P., Zwally, H. J., and Comiso, J. C.: Arctic sea ice extents, areas, and trends, 1978–1996, Journal of Geophysical Research: Oceans (1978–2012), 104, 20837-20856, 1999.

Pavlova, O., Pavlov, V., and Gerland, S.: The impact of winds and sea surface temperatures on the Barents Sea ice extent, a statistical approach, Journal of Marine Systems, 130, 248-255, 2014.

Peterson, B. J., Holmes, R. M., McClelland, J. W., Vörösmarty, C. J., Lammers, R. B., Shiklomanov, A. I., Shiklomanov, I.
505   A., and Rahmstorf, S.: Increasing river discharge to the Arctic Ocean, science, 298, 2171-2173, 2002.

Post, E., Bhatt, U. S., Bitz, C. M., Brodie, J. F., Fulton, T. L., Hebblewhite, M., Kerby, J., Kutz, S. J., Stirling, I., and Walker, D. A.: Ecological Consequences of Sea-Ice Decline, Science, 341, 519, 2013.

Prinsenberg, S. J.: On the physical oceanography of Foxe Basin. In: Elsevier oceanography series, Elsevier, 1986.

Rahmstorf, S.: Bifurcations of the Atlantic thermohaline circulation in response to changes in the hydrological cycle, Nature,
510   378, 145, 1995.

Rahmstorf, S. and Ganopolski, A.: Long-term global warming scenarios computed with an efficient coupled climate model, Climatic change, 43, 353-367, 1999.

Rao, A. R., Hamed, K. H., and Chen, H.-L.: Nonstationarities in hydrologic and environmental time series, Springer Science & Business Media, 2012.

515   Rennolls, K. and Wang, M.: A new parameterization of Johnson's SB distribution with application to fitting forest tree diameter data, Canadian Journal of Forest Research, 35, 575-579, 2005.

Rothrock, D. A., Yu, Y., and Maykut, G. A.: Thinning of the Arctic sea-ice cover, Geophysical Research Letters, 26, 3469-3472, 1999.

520   Rousset, C., Vancoppenolle, M., Madec, G., Fichefet, T., Flavoni, S., Barthélemy, A., Benshila, R., Chanut, J., Lévy, C., and Masson, S.: The Louvain-la-Neuve sea ice model LIM3. 5: global and regional capabilities, Geoscientific Model Development Discussions, 8, 2015.

Saucier, F., Senneville, S., Prinsenberg, S., Roy, F., Smith, G., Gachon, P., Caya, D., and Laprise, R.: Modelling the sea ice-ocean seasonal cycle in Hudson Bay, Foxe Basin and Hudson Strait, Canada, Climate Dynamics, 23, 303-326, 2004.

Schwarz, G.: Estimating the dimension of a model, The annals of statistics, 6, 461-464, 1978.

525   Serreze, M. C. and Barry, R. G.: Processes and impacts of Arctic amplification: A research synthesis, Global and Planetary Change, 77, 85-96, 2011.

Shokr, M. and Sinha, N.: Sea Ice: Physics and Remote Sensing, Wiley, 2015.

Smith, D.: Extraction of winter total sea-ice concentration in the Greenland and Barents Seas from SSM/I data, Remote Sensing, 17, 2625-2646, 1996.

530   Stocker, T.: Climate change 2013: the physical science basis: Working Group I contribution to the Fifth assessment report of the Intergovernmental Panel on Climate Change, Cambridge University Press, 2014.

Stroeve, J., Holland, M. M., Meier, W., Scambos, T., and Serreze, M.: Arctic sea ice decline: Faster than forecast, Geophysical research letters, 34, 2007.

Stroeve, J., Markus, T., Boisvert, L., Miller, J., and Barrett, A.: Changes in Arctic melt season and implications for sea ice
535   loss, Geophysical Research Letters, 41, 1216-1225, 2014.

Stroeve, J. C., Kattsov, V., Barrett, A., Serreze, M., Pavlova, T., Holland, M., and Meier, W. N.: Trends in Arctic sea ice extent from CMIP5, CMIP3 and observations, Geophysical Research Letters, 39, n/a-n/a, 2012.

Sulaiman, M. Y., Oo, W. H., Wahab, M. A., and Zakaria, A.: Application of beta distribution model to Malaysian sunshine data, Renewable energy, 18, 573-579, 1999.

540   Tonboe, R. T., Eastwood, S., Lavergne, T., Sørensen, A. M., Rathmann, N., Dybkjær, G., Pedersen, L. T., Høyer, J. L., and Kern, S.: The EUMETSAT sea ice concentration climate data record, The Cryosphere, 10, 2275-2290, 2016.

Vermaire, J. C., Pisaric, M. F., Thienpont, J. R., Courtney Mustaphi, C. J., Kokelj, S. V., and Smol, J. P.: Arctic climate warming and sea ice declines lead to increased storm surge activity, Geophysical Research Letters, 40, 1386-1390, 2013.

Wakazuki, Y.: Modified Relative Humidity Based on the Johnson's S_B Distribution Function, SOLA, 9, 111-
545   114, 2013.

Wald, A. and Wolfowitz, J.: On a Test Whether Two Samples are from the Same Population, doi: 10.1214/aoms/1177731909, 1940. 147-162, 1940.

Wang, J., Mysak, L. A., and Ingram, R. G.: Interannual variability of sea-ice cover in Hudson Bay, Baffin Bay and the Labrador Sea, Atmosphere-ocean, 32, 421-447, 1994.

550   Wang, M. and Overland, J. E.: A sea ice free summer Arctic within 30 years?, Geophysical research letters, 36, 2009.

Wassmann, P., Duarte, C. M., Agusti, S., and Sejr, M. K.: Footprints of climate change in the Arctic marine ecosystem, Global change biology, 17, 1235-1249, 2011.

Weaver, A. J., Eby, M., Wiebe, E. C., Bitz, C. M., Duffy, P. B., Ewen, T. L., Fanning, A. F., Holland, M. M., MacFadyen, A., Matthews, H. D., Meissner, K. J., Saenko, O., Schmittner, A., Wang, H., and Yoshimori, M.: The UVic earth system
555 climate model: Model description, climatology, and applications to past, present and future climates, Atmosphere-Ocean, 39, 361-428, 2001.

Wessel, P. and Smith, W. H. F.: A global, self-consistent, hierarchical, high-resolution shoreline database, Journal of Geophysical Research: Solid Earth, 101, 8741-8743, 1996.

Wilcoxon, F.: Individual Comparisons by Ranking Methods, Biometrics Bulletin, 1, 80-83, 1945.

560 Yao, A. Y. M.: A Statistical Model for the Surface Relative Humidity, Journal of Applied Meteorology, 13, 17-21, 1974.